Chem Soc Rev

Cell Surface-based Sensing with Metallic Nanoparticles

Journal:	*Chemical Society Reviews*
Manuscript ID:	CS-TRV-11-2014-000387.R2
Article Type:	Tutorial Review
Date Submitted by the Author:	18-Mar-2015
Complete List of Authors:	Jiang, Ziwen; University of Massachusetts--Amherst, Chemistry Le, Ngoc; University of Massachusetts--Amherst, Chemistry Gupta, Akash; University of Massachusetts--Amherst, Chemistry Rotello, Vincent M; University of Massachusetts at Amherst, Dept. of Chemistry (710A LGRT)

SCHOLARONE™
Manuscripts

1   **Cell Surface-based Sensing with Metallic Nanoparticles**

2   **Ziwen Jiang, Ngoc D. B. Le,[†] Akash Gupta,[†] Vincent M. Rotello***

3   Department of Chemistry, University of Massachusetts Amherst, 710 North Pleasant St, Amherst,

4   Massachusetts, MA 01003, USA

5   [†] These authors equally contributed to this work.

6

7   * Correspondence should be addressed to Vincent M. Rotello (V. M. R.).

8   **Address**:

9   Department of Chemistry

10   710 North Pleasant Street

11   University of Massachusetts

12   Amherst, MA 01003, USA.

13   **Tel.**: +1 413 545 2058; **fax**: +1 413 545 4490.

14   **E-mail**: rotello@chem.umass.edu.

15

16 **Abstract**

17   Metallic nanoparticles provide versatile scaffolds for biosensing applications. In this

18   review, we focus on the use of metallic nanoparticles for cell surface sensings. Examples of the

19   use of both specific recognition and array-based "chemical nose" approaches to cell surface

20   sensing will be discussed.

21

22   **Key learning points**

23   1. Both cell surface biomarkers (such as carbohydrates and proteins) and the overall cell surface

24   signatures provide crucial information for identifying cell types.

25   2. Metallic nanoparticles provide multiple modes of signal transduction for biosensing

26   applications.

27   3. Surface functionalization determines how nanoparticles interact with cell surfaces.

28   4. The specific recognition capabilities of biomacromolecules such as antibodies, lectins,

29   aptamers, and DNAzymes can be coupled with nanoparticle transduction processes to design cell

30   sensing strategies.

31   5. Nanoparticle surface can be functionalized with a variety of small molecule ligands to provide

32   the selective recognition required for array-based sensing.

33

34   **TOC**

35

36
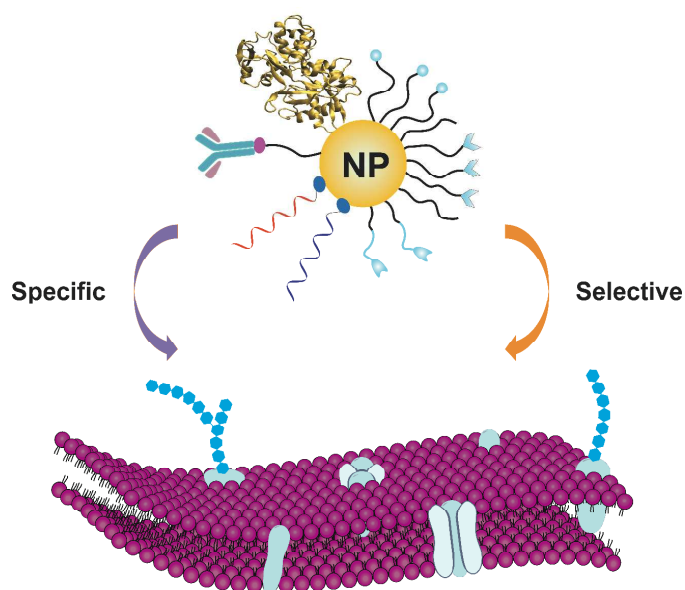
1. Introduction

Cell surface sensors for disease and detection of infection have direct access to the sensing target, in contrast to approached that detect intracellular proteins, nucleic acids, or other markers buried inside the cells. This ready access has the potential to provide rapid sensing with minimal processing. The rich environment presented by the cell exterior also gives cell surface sensors the capability to read out the phenotypes of cells, a property that is the final outcome of multiple factors including both genetic and epigenetic variations.[1] For example, in the case of cancer, abnormal cells have been found to overexpress specific glycosylated proteins at their plasma membrane such as epithelial cell adhesion molecule (EpCAM) or carcinoembryonic antigen (CEA).[2-4] Therefore, targeting cell surface phenotype provides a strategy for simple, rapid, and robust diagnostic pathways in diverse areas such as cancer and pathogenic bacteria.

Three integrated components are necessary to fabricate an effective sensor: (1) a recognition element to interact with a target analyte, (2) a signal transduction element to generate a measurable signal from an analyte-receptor binding event, and (3) a device that outputs a result. Metallic nanoparticles (NPs) can be easily engineered to provide scaffolds for recognition processes, with their physical properties facilitating the transduction process, making them excellent platforms for cell surface sensing.[5,6]

In this review, we will focus on the use of metallic NPs for the detection and quantification of cell properties, based on cell surface components. We will discuss examples of different engineered metallic NP systems[7,8] that provide cell sensing through specific and selective interactions with the cell surfaces.

2. Cell surface and nanoparticle interactions

Enormous cell surface diversity exists among cells from plants, bacteria, and animals. The surface of a mammalian cell is composed of a complex structure featuring the lipid bilayer, proteins, nucleic acids as well as a range of polysaccharide structures that comprise the glycocalyx.[9] This glycocalyx is composed of glycoproteins, proteoglycans and glycolipids.[10] Phenotypically altered expression of each of these components provides diagnostic information for diseases such as cancer, Gaucher's, and Tay-Sachs diseases.[11,12] Taken together, the complex

68   array of biomolecules that comprise cell surfaces make them excellent targets for both specific

69   biomarker sensing and selective "chemical nose" based methods.

70

71   The interaction between nanomaterials and cells is an important issue for designing

72   systems not only for sensing, but also for imaging and delivery. In general, the following factors

73   need to be taken into account: (1) specific receptors (biomarkers) on the cell membrane, (2) the

74   size, shape, surface charge, roughness and hydrophobicity of nanoparticles and their role in

75   selective interactions. While these topics are all central to the sensing described here, the in-

76   depth discussion required for understanding this interaction is beyond the scope of this tutorial

77   discussion. Nel and coworkers have provided a comprehensive review to help understand the

78   biophysicochemical interactions at the nano-bio interface, which discussed cell-nanoparticle

79   interactions in detail.[13]

80

81   **3. Specific sensing**

82   We will focus on spherical metallic nanoparticles in this review, as these systems have

83   been widely employed for cell surface sensing. Metallic nanoparticles can be functionalized with

84   small molecules [14] and biomacromolecules [15] to achieve the specific interactions with the

85   biological targets. However, the vast majority of specific-based sensors have been using

86   biomacromolecules to functionalize metallic nanoparticles, so we will focus on these

87   bioconjugate systems. These platforms provide highly adaptable tools for rapid and/or point-of-

88   care tools that provide alternatives to more complex and instrument-intensive techniques such as

89   flow cytometry. [16]

90

91   **3.1. Antibody-based sensing**

92   Antibodies are widely used as recognition elements in diagnostic and therapeutic

93   applications.[17] There are two key components of antibodies: the Fab (fragment, antigen-binding)

94   region of an antibody that recognizes the antigen and the Fc (fragment, constant) that can be used

95   for conjugation without disrupting the recognition process. Conjugation of either complete

96   antibodies or Fab fragments to NPs provides an effective means of recognizing cell surface

97   functionality. As described below, these binding events can be detected *via* various tools such as

98   surface-enhanced Raman scattering (SERS) and electrochemistry.

99

100   SERS is a technique in which the Raman signal can be dramatically amplified through

101   surface plasmon resonance of metallic NPs.[6] SERS-based techniques utilizing antibodies have

102   been successfully applied to immunoassay-based methodologies.[18] In one example, Sha and

103   coworkers detected cancer circulating cells (CTCs) by combining capturing capability of a

104   magnetic bead and specific labeling of SERS nanotags.[19] This bead was conjugated with anti-

105   EpCAM antibody to capture SKBR3 cancer cells. These cells were then labeled for SERS

106   detection by AuNPs functionalized with anti-HER2 antibody (human epidermal growth factor

107   receptor-2). A silica shell was subsequently coated on this complex to enable the

108   functionalization of antibody on the particle without interfering with the Raman response (Figure

109   1). In a similar study, SERS-based systems were further employed for *in vivo* tumor targeting.

110   Poly(ethylene glycol)-capped AuNPs were used to stabilize Raman-active reporter molecules.

111   The SERS-NPs were conjugated with antibodies specifically targeting the overexpressed

112   epidermal growth factor receptor on tumor cells, resulting in highly specific *in vivo* tumor

113   detection.[20]
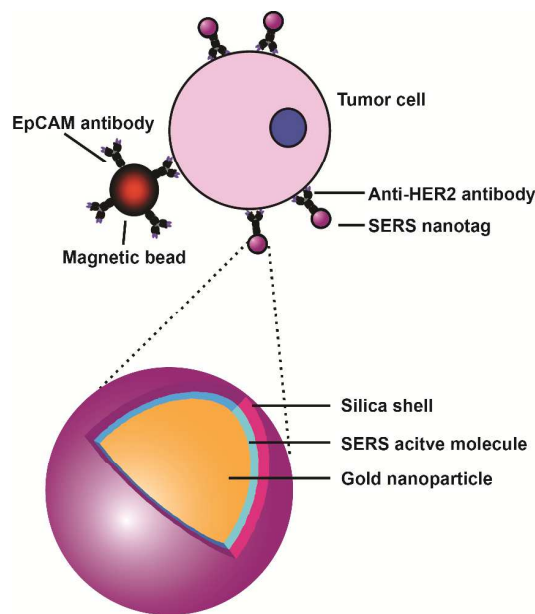
114

115   **Figure 1** Tumor cell detection using anti-HER2 antibody-conjugated magnetic beads with SERS

116   nanotags. Reprinted with permission from ref. 19. Copyright 2008 American Chemical Society.

117

118   Electrochemical detection technique can utilize the electrocatalytic properties of AuNPs

119   to provide rapid cell surface sensing.[21] This strategy has the advantages of simpler

120   instrumentation coupled with the direct connection of sensor output with devices/computers. For

121   example, Merkoçi and coworkers employed antibody-conjugated magnetic beads and AuNPs for

122   the detection of CTC (Figure 2).[22] AuNPs fabricated with anti-EpCAM antibody were used for

123   targeting EpCAM, an overexpressed transmembrane glycoprotein on human colon

124   adenocarcinoma cells (Caco2 cells). The AuNP-antibody conjugates were used to generate an

125   electrochemical signal through electrocatalytic hydrogen evolution. The signals generated from

126   AuNP-antibody conjugates could detect 2.2×10^2 Caco2 cells in the presence of other interfering

127   cells such as monocytes (THP-1).

128
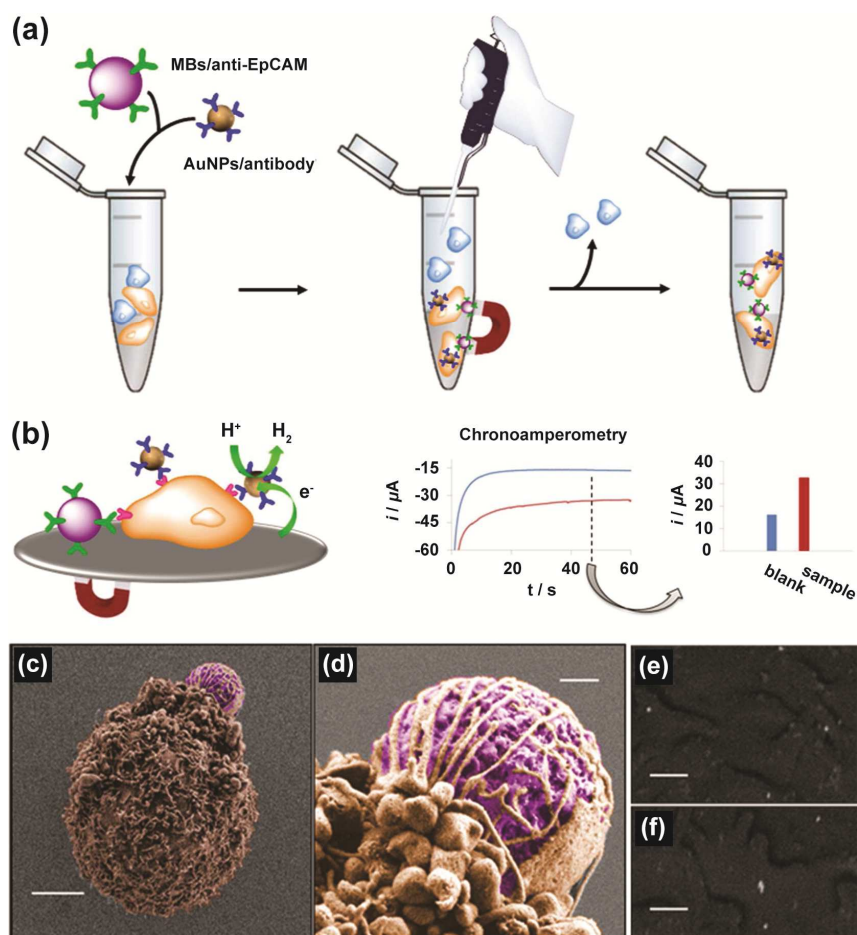
129

130   **Figure 2** (a) Capture of Caco2 cells by magnetic beads conjugated to anti-EpCAM.

131   Simultaneously, cells were labeled with AuNP-specific antibodies in the presence of interfering

132   cells (THP-1). (b) Chronoamperometry of the hydrogen evolution reaction (HER)

133   electrocatalyzed by AuNPs. (c), (d) False colors scanning electron microscopy (SEM) images of

134   a Caco2 cell captured by magnetic beads (MBs)/anti-EpCAM. (e), (f) Backscattered images

135   showing AuNPs distributed along the cell plasma membrane of Caco2 cells. Scale bars, 3 μm (c),

136   400 nm (d), and 200 nm (e, f). Reprinted with permission from ref. 22. Copyright 2012

137   American Chemical Society.

138

139   **3.2. Lectin-based sensing**

140   Lectins are proteins that exhibit strong and specific or selective binding towards

141   carbohydrate moieties. Targeting carbohydrates has been the useful strategy for diagnosis

142   because the alterations of carbohydrates found on plasma membrane have been correlated with

143   disease, such as liver fibrosis, pancreatic cancer, and cervical cancers.[23] Thus, NPs

144   functionalized with lectins can be a powerful tool for cell surface sensing.[24]

145

146   In a recent study, Liu and coworkers designed a sensitive electrochemiluminescence[25]

147   (ECL)-based biosensor using a displacement assay that relies on the interaction between NP-

148   bound lectins and carbohydrates on the cell surface (Figure 3).[26] In this system, a gold electrode

149   immersed in luminol solution was coated with Concanavalin A (ConA), a lectin that recognizes

150   mannose (a carbohydrate type found on the cell surface). These mannose moieties can also be

151   found in glucose oxidase molecules (GOx), an enzyme that can catalyze the luminol ECL

152   reaction. By coupling GOx with AuNPs (GOx-Au), they were able to fabricate a multifunctional

153   probe. This GOx-Au probe can both compete with mannose moieties on the analyte cells for

154   ConA-coated gold electrode and improve the ECL signal of luminol. In the presence of the target

155   cells, the competition between GOx-Au and mannose-containing cells generates the alterations in

156   ECL signal intensity, providing the ability to profile carbohydrate-lectin interaction and *in situ*

157   cell surface carbohydrate expression.

158

159

160
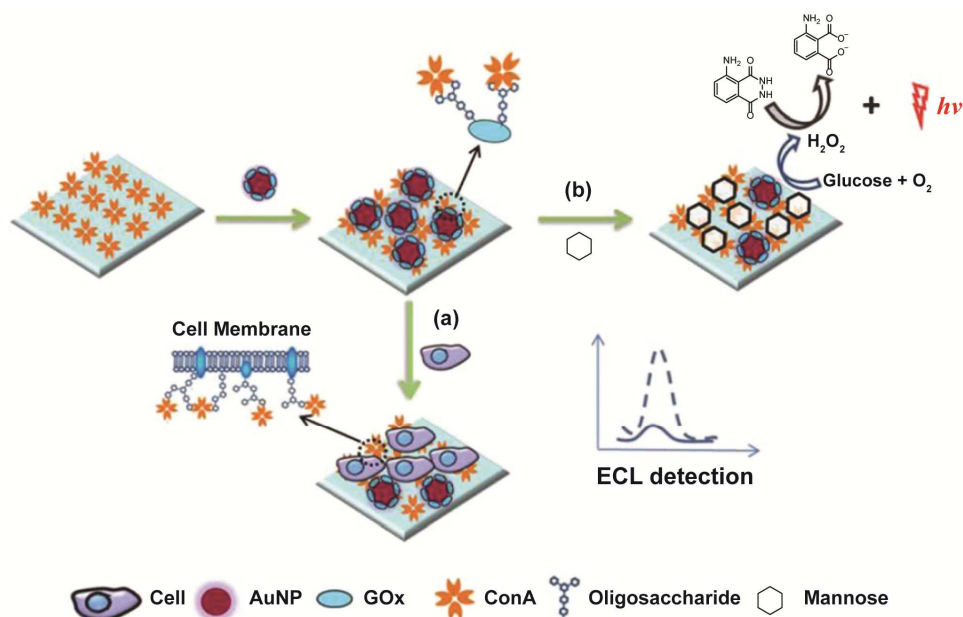
Figure 3 Schematic illustration of the lectin-based sensing strategy for (a) carbohydrate-ConA interaction analysis and (b) cell surface carbohydrate expression. Reprinted with permission from ref. 26. Copyright 2013 Royal Society of Chemistry.

3.3. Aptamer-based sensing

Short, single-stranded oligonucleotides (ssDNA or ssRNA), known as aptamers, provide an emerging strategy for biorecognition. Aptamers are produced from an *in vitro* method known as SELEX (systematic evolution of ligands by exponential enrichment). In this process, SELEX uses polymerase chain reaction (PCR) to specifically amplify the sequence that has high affinity and selectivity to the target analyte. The iterative process generates aptamers that often fold into unique three-dimensional conformations. Aptamers can bind to target molecules ranging from small organic molecules to biomacromolecules,[27] making them promising candidates to serve as recognition elements in biosensors.

The recognition capabilities of aptamers can be combined with the spectroscopic advantages of AuNPs for cell detection applications. AuNPs possess strong distance dependent optical properties due to surface plasmon resonance.[28] The aggregation of aptamer-conjugated AuNPs causes a shift in their absorption spectra, resulting in a change in their scattering profile and color from red to blue/purple.[29] This colorimetric sensing method has been applied using aptamers for the detection of cancer cells. For instance, Tan and coworkers successfully applied

182　the aggregation-based colorimetric sensing platform to detect cancer cells using AuNPs

183　functionalized with the aptamers of interest.[30] The specific interaction between AuNP-aptamer

184　conjugates and the target cells (CCRF-CEM acute leukemia cell) induced a distinct color change

185　(Figure 4).
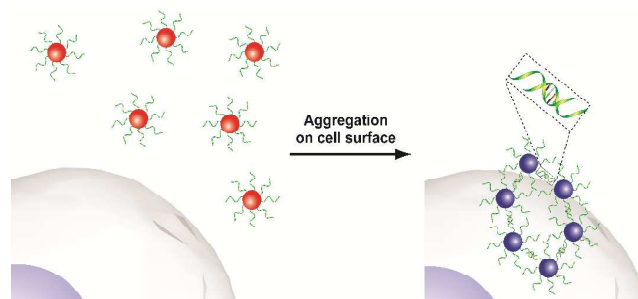
186

187　**Figure 4** Aptamer-conjugated gold nanoparticles used in colorimetric sensing of cancer cells.

188

189　　　　Recently, DNA-templated silver nanoclusters (DNA-AgNCs) were used as a signal

190　transduction element for use with aptamers. The fluorescence of DNA-AgNCs can be

191　significantly amplified in proximity of guanine-rich DNA sequences, [31] a phenomena Wang and

192　coworkers have applied in cell surface-based sensing.[32] They designed a "turn-on" system for

193　cancer cell detection, utilizing the fluorescence enhancement of DNA-AgNCs and the

194　recognition capability of aptamers. Two separate DNA-based probes were involved in this

195　system, denoted as the recognition probe and signal probe. The recognition probe was designed

196　as a hairpin-shaped structure that contains a CCRF-CEM cancer cell specific aptamer sequence,

197　a guanine-rich DNA sequence and an arm segment. The signal probe contains a sequence for

198　AgNC-templated synthesis and a link sequence that is complementary to the arm segment of the

199　recognition probe. Once the aptamer sequence from the recognition probe recognizes and binds

200　to CCRF-CEM cells, the recognition probe undergoes a conformational alteration. This

201　conformational alternation then initiates the hybridization of the two probes and consequently

202　brings DNA-AgNCs close to the guanine-rich DNA sequence, resulting in an enhanced

203　fluorescence readout (Figure 5).
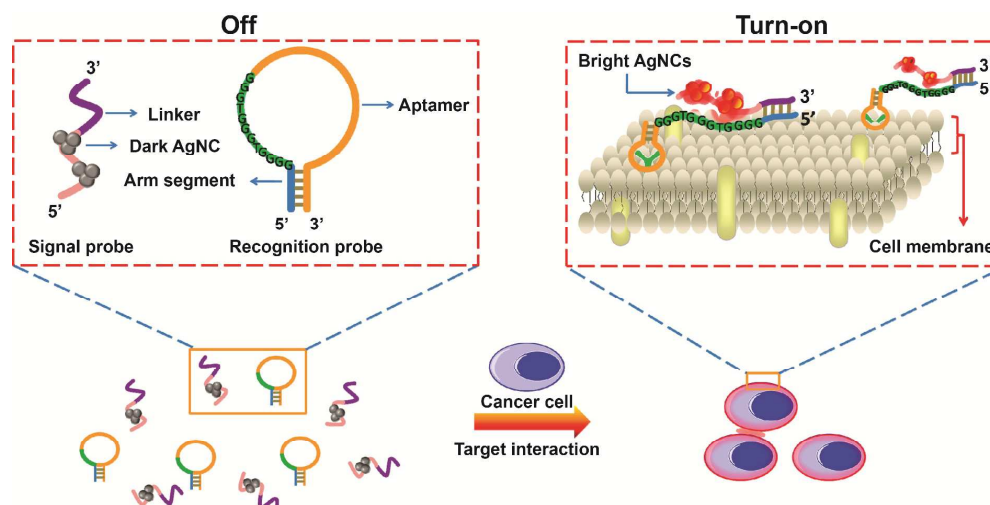
204

205 **Figure 5** Schematic representation of cancer cell detection based on DNA-templated silver

206 nanoclusters (AgNCs). Reprinted with permission from ref. 32. Copyright 2013 American

207 Chemical Society.

208

209 Aptamer-based specific sensing can also be used to detect different cancer cells using an

210 electrochemical approach. By combining multiple metallic NPs with electrochemical analysis,

211 Kelley and coworkers designed a chip-based strategy for the analysis of cancer cells associated

212 with different tumor phenotypes.[33] Pd, Ag, and Cu NPs were chosen as signal reporters since

213 they have well-separated potentials as redox-active probes. Biomarker-specific aptamers were

214 conjugated with these three types of metallic NPs to form Pd-anti-PSMA, Ag-anti-HER2, and

215 Cu-anti-MUC1 NPs. A mixture of these three NPs were successfully used for the specific

216 detection of different prostate and breast cancer cell lines such as VCaP, SK-BR-3, and MDA-

217 MB-231 (Figure 6).
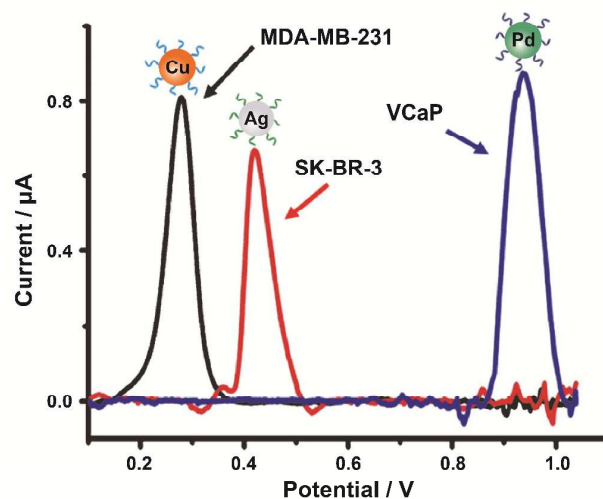
218

219   **Figure 6** Linear-sweep voltammetry of specific cancer cell detection with a mixture of Pd-anti-

220   PSMA, Cu-anti-MUC1, and Ag-anti-HER2 nanoparticles: VCaP (blue), MDA-MB-231 (black)

221   and SK-BR-3 (red) cells. Reprinted with permission from ref. 33. Copyright 2014 WILEY-VCH

222   KGaA, Weinheim.

223

224   **3.4. DNAzyme-based sensing**

225   Deoxyribozymes, known as DNAzymes or catalytic DNAs, provide an alternative

226   approach to biosensing. DNAzymes are selected from random DNA sequences through

227   combinatorial screening techniques for catalytic and ligand-binding activities.[34] DNAzyme-

228   based sensing relies on the optical property of AuNPs for target recognition role for analytes

229   such as as metal ions and small organic molecules. Using such DNAzyme-functionalized AuNPs,

230   the DNAzyme-catalyzed cleavage or ligation of the nucleic acid substrates affects the assembly

231   of AuNPs, resulting in a colorimetric readout for the cofactors.[34]

232

233   DNAzymes can also be used for signal amplification by behaving as peroxidase mimics.

234   For example, it has been found that when one certain DNA sequence binds with hemin,

235   DNAzyme can be formed with G-quadruplex motifs. This type of DNAzyme can catalyze the

236   generation and enhancement of chemiluminescence (CL) signals in the presence of luminol and

237   H_2O_2. In this process, AuNPs are employed as carriers for these horseradish peroxidase (HRP)-

238   mimicking DNAzymes.[35] In a recent study, Zhang and coworkers applied HRP-mimicking

239   DNAzyme-functionalized NPs to cancer cell detection through the amplified CL signals.[36]

240

4. Selective sensing

Specific recognition-based sensors require pre-identification of the biomarkers, and face certain limitations when used in systems containing multiple analytes. For example, cancer cells present multiple biomarkers on the cell surface. The level of biomarkers may vary among cell populations. In addition, subtle changes in the biomarker levels may be indicative of dramatic phenotypic differences. As an alternative, sensors using *selectivity*-based modality do not require the knowledge of a specific biomarker. On the contrary, selectivity-based approaches capture the responses from complex analytes to generate a signature for each sample. Such selective sensing approach can be utilized to detect non-specific analytes with either a single recognition element or more commonly an array of recognition elements. In a typical array-based sensor, a set of recognition elements interacts with a number of different analytes or classes of analytes, providing a process reminiscent of mammalian olfaction.[37] This mechanistic similarity is why array-based sensors are often denoted as chemical "noses" or "tongues".

254

4.1. Single recognition element system

Rotello and coworkers have developed an enzyme amplification sensor using cationic AuNP to inhibit the activity of β-galactosidase (β-gal) based on electrostatic interaction.[38] Such enzyme catalysis can amplify the weak signals generated by the system. Bacterial cell surfaces are negatively charged which can disrupt the AuNP-β-gal conjugates. During the sensing process, bacteria cells replace β-gal from the NP-β-gal conjugates, restoring the activity of β-gal towards the chromogenic substrate. Finally, the enzymatic reaction on the substrate gives the corresponding readout to quantify the analytes (Figure 7).[39] The enzyme-amplified colorimetric readout was able to detect 10^2 CFU/mL of *Escherichia coli* (*E. coli*) in solution. Furthermore, the performance of this methodology was tested on a paper strip format against concentrations of bacteria ranging from $10^4 \sim 10^8$ CFU/mL. The designed bacteria test strips demonstrate the potential for field applications such as a test of drinking water safety. However, this strategy displays limitations in sensitivity and multiple analyte detection capability due to insufficient interactions between the single recognition element and the analytes.
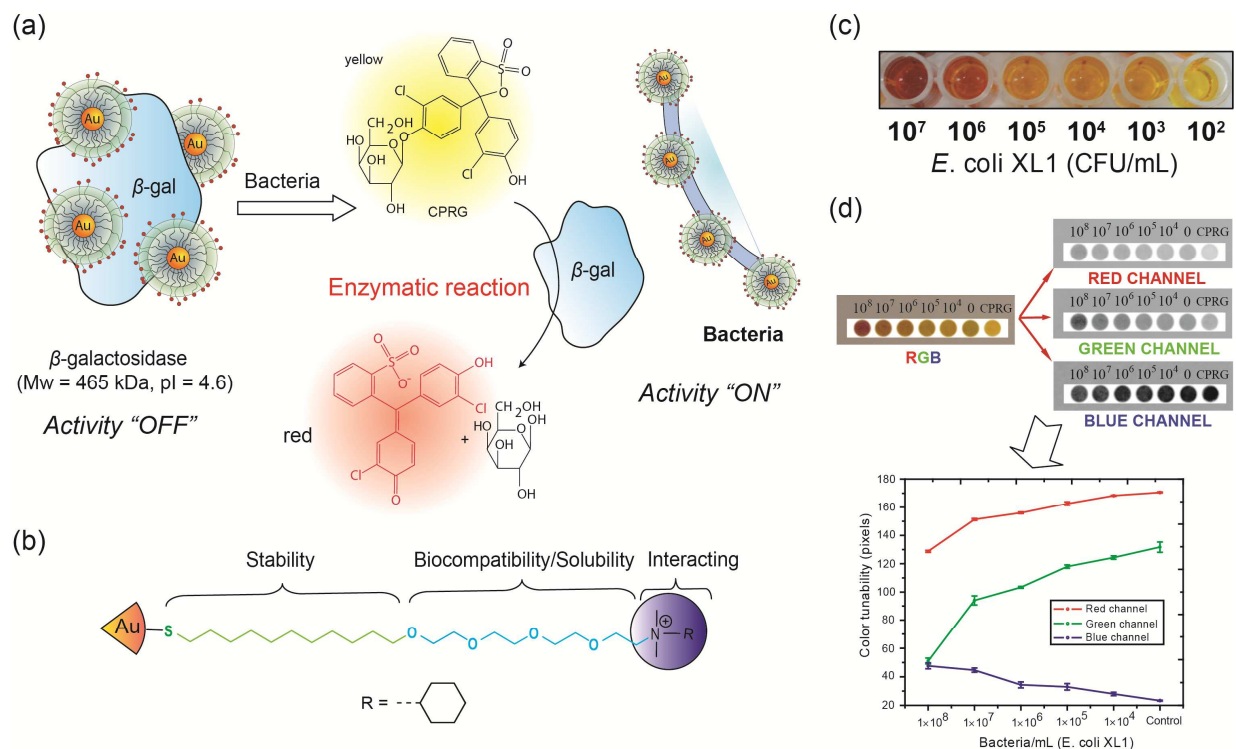
Figure 7 (a) Schematic demonstration of enzyme amplified sensing of bacteria using gold nanoparticles. (b) The structure of quaternary amine functionalized gold nanoparticles. (c) The colorimetric sensing of *Escherichia coli* (*E. coli*) in solution. (d) Schematic illustration of the RGB analysis for monitoring color changes on test strips for different concentrations of *E. coli*. Reprinted with permission from ref. 39. Copyright 2011 American Chemical Society.

4.2. Array based sensing systems

Multiple recognition elements can maximize the variation in interactions between sensors and analytes. This array-based strategy combines responses from many individual sensors and analytes to generate a distinct pattern (fingerprint) for each analyte, either based on specific or selective interactions. Since multiple responses can be obtained from array-based sensors, these data matrices are generally analyzed using a variety of multivariate analyses such as principal component analysis (PCA) or linear discriminant analysis (LDA).[40]

NPs can be readily functionalized with ligands to generate diverse sensor elements. These head groups exhibit differential affinity towards various analytes, leading to variations in the sensor that can be correlated to cellular signatures. Rotello and coworkers have designed several

287   small molecule based sensor arrays that used the phenomenon of fluorescence quenching.[41]

288   Fluorescence quenching is reduction in the fluorescence quantum yield due to energy transfer

289   from the photo-excited fluorophore to the AuNPs. In one approach, gold nanoparticles (AuNPs)

290   with a fluorescent polymer [carboxylate poly(para-phenyleneethynylene) (PPE-CO_2)] were used

291   to discriminate a series of cell lines (Figure 8).[42] The sensor was comprised of three NP types

292   with different quaternary amine functional head groups. An array of AuNPs was used to quench

293   the intensity of the fluorescent polymers *via* electrostatic interaction. The subsequent binding of

294   cells disrupted the AuNP-polymer complex, thereby generating different fluorescence response

295   patterns for each cell lines. This AuNP-polymer complex was able to identify human cancerous

296   (MCF-7), metastatic (MDA-MB231) and normal (MCF10A) breast cell lines. Since these cell

297   lines came from different individuals, their differentiation might be originating from genetic

298   variation. To avoid this possibility, isogenic cell lines [CDBgeo (normal), TD (cancerous) and

299   V14 (metastatic)] derived from BALB/c mice were used to validate the sensor. Fluorescent

300   proteins can also be used as a transducer in an array based sensor. Cell differentiation using

301   AuNP-green fluorescent protein (GFP) conjugates resulted in four-fold enhancement in the

302   sensitivity of "chemical nose"-based sensor.[43] Moreover, in a subsequent study, AuNP-GFP

303   constructs were used to discriminate site specific metastases and healthy state using cell lysates

304   as well as tissue lysates, providing a promising strategy for medical diagnosis.[44]

305

306

307
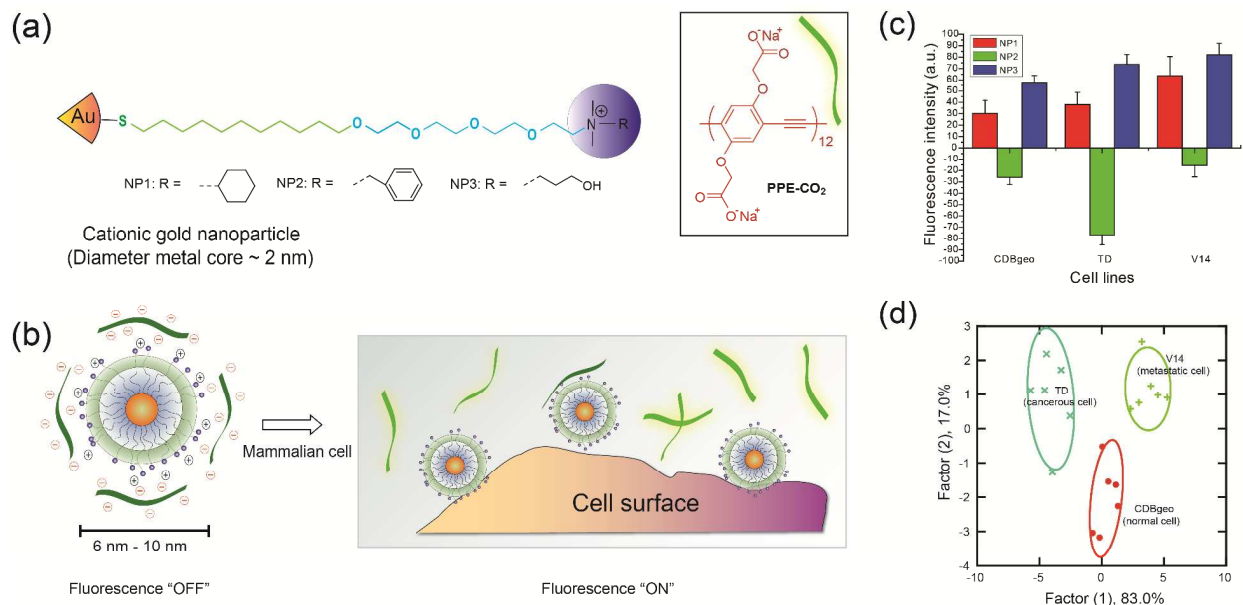
Figure 8 (a) Cationic gold nanoparticles (NP1-NP3) and the fluorescent polymer, carboxylate poly(para-phenyleneethynylene) (PPE-CO2). (b) Fluorescence quenching of the polymers and the restoration of fluorescence after AuNP-polymer complex disrupted by the incubation with cells (dark green strips, fluorescence off; light green strips, fluorescence on). (c) Detection of three isogenic mammalian cell lines (CDBgeo, TD cell and V14) determined by fluorescence change using nanoparticle-polymer supramolecular complexes. (d) Canonical score plot using linear discrimination analysis (LDA) for the first two factors of simplified fluorescence response patterns obtained with NP-polymer assembly arrays against isogenic cell types. Reprinted with permission from ref. 42. Copyright 2009 National Academy of Sciences, USA.

In an analogous study, a swallowtail substituted carboxylate PPE (Sw-CO$_2$) was used as a transducer for AuNP-polymer sensor. [45] This array-based system comprised of amine functionalized hydrophobic NPs that served as recognition units for microorganisms such as bacteria. Bacterial cell walls are negatively charged and furnish a polyvalent environment to interact selectively with AuNP-polymer complex. For example, the Gram-positive microorganisms are highly negatively charged due to the presence of techoic acid residue, whereas *E. coli* bacteria possess pili (rich in lectins) emanating from the surface. This array-based sensor enables the detection of bacteria cells within minutes. The AuNP-polymer complex was disrupted *via* competitive binding of different bacteria strains with the AuNP. Twelve

328   different bacteria strains including Gram-positive strains such as *Bacillus subtilis*, *Amycolatopsis*

329   *azurea* and Gram-negative bacteria such as *E. coli*, and *Pseudomonas putida* were identified.

330

331   Recently, quantum dots (QDs) were used in an array-based sensor as a recognition

332   element alongside AuNPs. When added together to the cells, co-localization of AuNPs and QDs

333   resulted in quenching, generating different patterns based on cell type/state. This sensor was used

334   to differentiate four different types of cancer cells as well as isogenic normal, cancer and

335   metastatic cells (Figure 9).[46] The dual channel fluorescence response obtained from the QD-

336   AuNP sensor array could identify 30 unknown samples with 100% accuracy. Besides pairing

337   with QDs, AuNPs can also be combined with upconversion nanoparticles (UCNPs) as a

338   fluorescence resonance energy transfer (FRET) couple to design biosensors.[47]
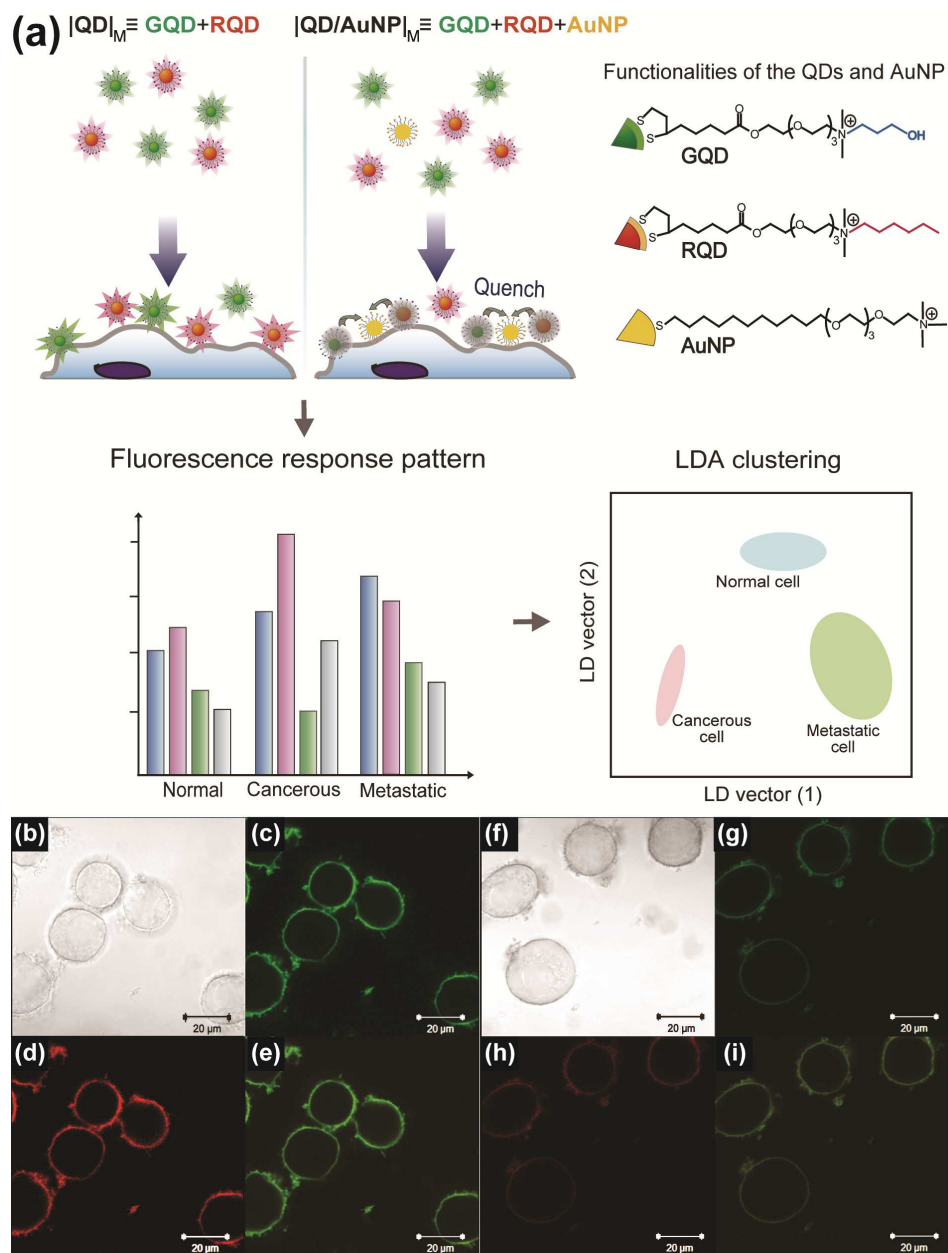
Figure 9 (a) Schematic illustration of the interaction between the nanoparticles and cell surface. The sensing system generated differential quenching and provided distinct patterns to discern different types/states of cells. Two arrays ($|QD|_M$ and $|QD/AuNP|_M$) were used in the system and placed in separated wells, with each array providing two fluorescence responses. $|QD|_M$, the mixture of GQD and RQD; $|QD/AuNP|_M$, the mixture of GQD, RQD, and AuNP. (b)-(i) Confocal microscopy images of (b)-(e) $|QD|_M$ and (f)-(i) $|QD/AuNP|_M$ after the incubation with HeLa cells for 15 min: (b), (f) bright field; (c), (g) green channel; (d), (h) red channel; (e), (i) merged images. Reprinted with permission from ref. 46. Copyright 2013 Elsevier.

348

349   Functionalization of biomolecules such as aptamers on NPs can also be used for selective

350   identification of target analytes. Aptamers with selective binding properties towards were coated

351   on citrate capped AuNPs.[48] Upon addition of the target cells, aptamer-protected AuNPs

352   displayed different aggregation, generating different color patterns. Human cancer cells (Jurkat,

353   Reh, Raji) and normal human cells (WIL2-S) were distinguished with the array-based approach

354   by using one human immunoglobulin E aptamer (HIgE-1) and two thrombin aptamers (Tro-1

355   and Tro-2).

356

357   **4.3. Multiplexed output sensing system**

358   The previous array-based sensing examples use separate recognition elements to generate

359   the multiple sensor outputs required for identification of analytes. An alternative strategy to

360   generating information-rich data would be to use a single recognition element with multiple

361   outputs. Very recently, Rotello and coworkers have developed a high-throughput multi-channel

362   sensor that classifies the mechanism of chemotherapeutic drugs in minutes.[49] This sensor

363   consists of a single AuNP complexed with three different fluorescent proteins (FPs) that is used

364   to sense drug-induced physicochemical changes on cell surfaces. In the presence of cells,

365   differential displacement of the fluorophores with concomitant fluorogenesis provide a

366   ratiometric output that is measurable from a single readout (Figure 10). This result demonstrates

367   the ability of cell surface sensing to be used for high throughput screening of therapeutics, and

368   suggests the utility of these sensors for applications in toxicology and related fields.

369
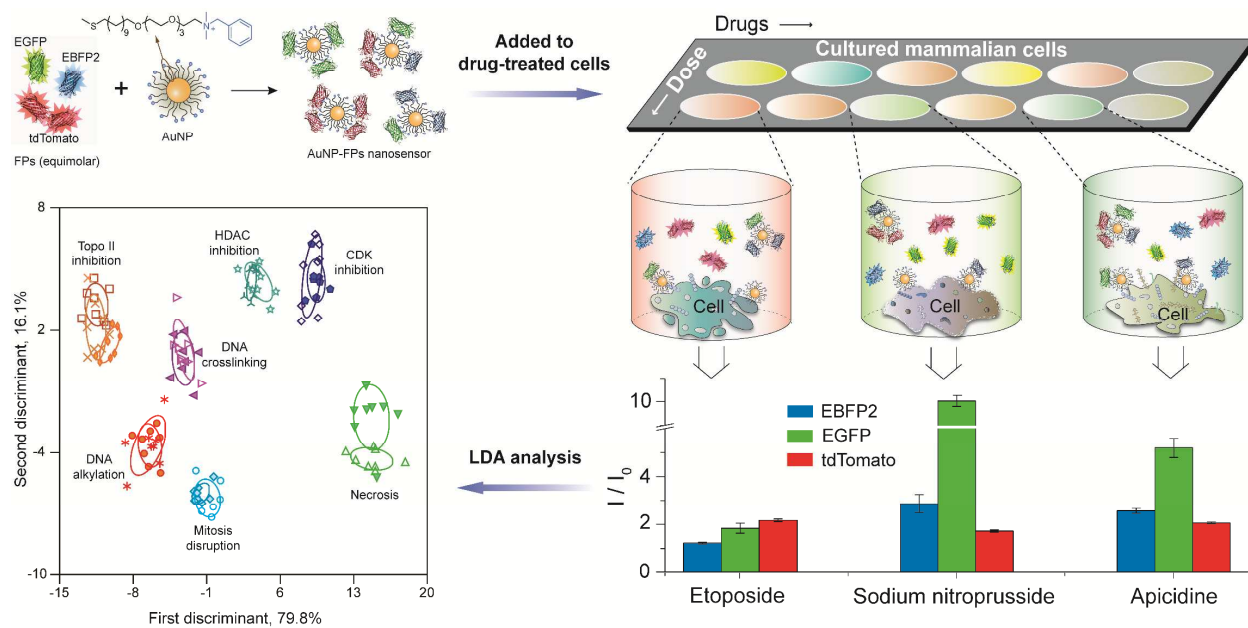
Figure 10 Multi-channel sensor fabricated by incubating AuNP to an equimolar mixture of three fluorescent proteins (FPs): tdTomato (red), EBFP2 (blue) and EGFP (green). Different drug-treated cells result in distinct cell surface phenotypes, leading to different FP displacement patterns as schematically shown for the three wells. The bar plot shows differential fluorescence responses for three representative drugs. These fluorescence responses were further analyzed by linear discriminant analysis (LDA) to generate different clusters corresponding to different categories of drug mechanisms. Each ellipse represents each drug in that mechanism category. Adapted with permission from ref. 49. Copyright 2014 by Nature Publishing Group.

5. Conclusions and prospects

Metallic NPs present a versatile platform for the creation of recognition elements for analyzing the biological targets. NPs can be fabricated with different recognition elements to provide specific or selective interactions with the target analytes. Moreover, physiochemical properties of the NPs such as fluorescence quenching or enhancement, surface enhanced Raman scattering and electrochemical activity can be harnessed to signal the transduction of the binding events. Hence, inclusion of NPs can simplify the system design as well as increase the sensitivity of the biosensors.

Incorporation of metallic nanoparticles in diagnostic techniques has opened promising avenues for a wide range of sensing strategies that feature combinations of simplicity, rapid

391 output, low cost platforms and multiplexing. As we develop better strategies for particle

392 functionalization and signal transduction, a wide range of platforms ranging from microfluidic

393 sensors through inexpensive paper test strips will be enabled, provide solutions to address health

394 issues worldwide.

395

396 **Acknowledgment**

401

402 **References**

1 H. Shen and P. W. Laird, *Cell*, 2013, **153**, 38-55.

2 M. Ferrari, *Nat. Rev. Cancer*, 2005, **5**, 161-171.

3 L. Harris, H. Fritsche, R. Mennel, L. Norton, P. Ravdin, S. Taube, M. R. Somerfield, D. F. Hayes and R. C. Bast, Jr., *J. Clin. Oncol.*, 2007, **25**, 5287-5312.

4 M. Trzpis, P. M. J. McLaughlin, L. M. F. H. de Leij and M. C. Harmsen, *Am. J. Pathol.*, 2007, **171**, 386-395.

5 P. K. Jain, X. H. Huang, I. H. El-Sayed and M. A. El-Sayed, *Acc. Chem. Res.*, 2008, **41**, 1578-1586.

6 R. A. Sperling, P. Rivera Gil, F. Zhang, M. Zanella and W. J. Parak, *Chem. Soc. Rev.*, 2008, **37**, 1896-1908.

7 E. Katz and I. Willner, *Angew. Chem. Int. Ed.*, 2004, **43**, 6042-6108.

8 R. Mout, D. F. Moyano, S. Rana and V. M. Rotello, *Chem. Soc. Rev.*, 2012, **41**, 2539-2544.

9 M. Edidin, *Nat. Rev. Mol. Cell Biol.*, 2003, **4**, 414-418.

10 M. D. Mager, V. LaPointe and M. M. Stevens, *Nat. Chem.*, 2011, **3**, 582-589.

11 D. H. Dube and C. R. Bertozzi, *Nat. Rev. Drug Discov.*, 2005, **4**, 477-488.

12 K. Ohtsubo and J. D. Marth, *Cell*, 2006, **126**, 855-867.

13 A. E. Nel, L. Maedler, D. Velegol, T. Xia, E. M. V. Hoek, P. Somasundaran, F. Klaessig, V. Castranova and M. Thompson, *Nat. Mater.*, 2009, **8**, 543-557.

14 J. Sudimack and R. J. Lee, *Adv. Drug Del. Rev.*, 2000, **41**, 147-162.

15 N. L. Rosi and C. A. Mirkin, *Chem. Rev.*, 2005, **105**, 1547-1562.

16 N. Rifai, M. A. Gillette and S. A. Carr, *Nat. Biotechnol.*, 2006, **24**, 971-983.

17 P. Holliger and P. J. Hudson, *Nat. Biotechnol.*, 2005, **23**, 1126-1136.

18 M. D. Porter, R. J. Lipert, L. M. Siperko, G. Wang and R. Narayanana, *Chem. Soc. Rev.*, 2008, **37**, 1001-1011.

19 M. Y. Sha, H. Xu, M. J. Natan and R. Cromer, *J. Am. Chem. Soc.*, 2008, **130**, 17214-17215.

20 X. Qian, X.-H. Peng, D. O. Ansari, Q. Yin-Goen, G. Z. Chen, D. M. Shin, L. Yang, A. N. Young, M. D. Wang and S. Nie, *Nat. Biotechnol.*, 2008, **26**, 83-90.

21 E. Katz, I. Willner and J. Wang, *Electroanalysis*, 2004, **16**, 19-44.

22 M. Maltez-da Costa, A. de la Escosura-Muniz, C. Nogues, L. Barrios, E. Ibanez and A. Merkoci, *Nano Lett.*, 2012, **12**, 4164-4171.

23 R. Jelinek and S. Kolusheva, *Chem. Rev.*, 2004, **104**, 5987-6016.

24 L. Ding, W. Cheng, X. Wang, S. Ding and H. Ju, *J. Am. Chem. Soc.*, 2008, **130**, 7224-7225.

25 L. Hu and G. Xu, *Chem. Soc. Rev.*, 2010, **39**, 3275-3304.

26 Y. Wang, Z. Chen, Y. Liu and J. Li, *Nanoscale*, 2013, **5**, 7349-7355.

27 X. Fang and W. Tan, *Acc. Chem. Res.*, 2010, **43**, 48-57.

28 S. Srivastava, B. L. Frankamp and V. M. Rotello, *Chem. Mater.*, 2005, **17**, 487-490.

29 J. Liu and Y. Lu, *Nat. Protoc.*, 2006, **1**, 246-252.

30 C. D. Medley, J. E. Smith, Z. Tang, Y. Wu, S. Bamrungsap and W. Tan, *Anal. Chem.*, 2008, **80**, 1067-1072.

31 H.-C. Yeh, J. Sharma, J. J. Han, J. S. Martinez and J. H. Werner, *Nano Lett.*, 2010, **10**, 3106-3110.

32 J. Yin, X. He, K. Wang, F. Xu, J. Shangguan, D. He and H. Shi, *Anal. Chem.*, 2013, **85**, 12011-12019.

33 Y. Wan, Y.-G. Zhou, M. Poudineh, T. S. Safaei, R. M. Mohamadi, E. H. Sargent and S. O. Kelley, *Angew. Chem. Int. Ed.*, 2014, **53**, 13145-13149.

34 J. Liu, Z. Cao and Y. Lu, *Chem. Rev.*, 2009, **109**, 1948-1998.

35 T. Niazov, V. Pavlov, Y. Xiao, R. Gill and I. Willner, *Nano Lett.*, 2004, **4**, 1683-1687.

36 S. Bi, J. Zhang and S. Zhang, *Chem. Commun.*, 2010, **46**, 5509-5511.

37 N. D. B. Le, M. Yazdani and V. M. Rotello, *Nanomedicine*, 2014, **9**, 1487-1498.

38 O. R. Miranda, H.-T. Chen, C.-C. You, D. E. Mortenson, X.-C. Yang, U. H. F. Bunz and V. M. Rotello, *J. Am. Chem. Soc.*, 2010, **132**, 5285-5289.

39 O. R. Miranda, X. Li, L. Garcia-Gonzalez, Z.-J. Zhu, B. Yan, U. H. F. Bunz and V. M. Rotello, *J. Am. Chem. Soc.*, 2011, **133**, 9650-9653.

40 A. M. Martinez and A. C. Kak, *IEEE Trans. Pattern Anal.*, 2001, **23**, 228-233.

41 U. H. F. Bunz and V. M. Rotello, *Angew. Chem. Int. Ed.*, 2010, **49**, 3268-3279.

42 A. Bajaj, O. R. Miranda, I.-B. Kim, R. L. Phillips, D. J. Jerry, U. H. F. Bunz and V. M. Rotello, *Proc. Natl. Acad. Sci. U. S. A.*, 2009, **106**, 10912-10916.

43 A. Bajaj, S. Rana, O. R. Miranda, J. C. Yawe, D. J. Jerry, U. H. F. Bunz and V. M. Rotello, *Chem. Sci.*, 2010, **1**, 134-138.

44 S. Rana, A. K. Singla, A. Bajaj, S. G. Elci, O. R. Miranda, R. Mout, B. Yan, F. R. Jirik and V. M. Rotello, *ACS Nano*, 2012, **6**, 8233-8240.

45 R. L. Phillips, O. R. Miranda, C.-C. You, V. M. Rotello and U. H. F. Bunz, *Angew. Chem. Int. Ed.*, 2008, **47**, 2590-2594.

46 Q. Liu, Y.-C. Yeh, S. Rana, Y. Jiang, L. Guo and V. M. Rotello, *Cancer Lett.*, 2013, **334**, 196-201.

47 L. Y. Wang, R. X. Yan, Z. Y. Hao, L. Wang, J. H. Zeng, J. Bao, X. Wang, Q. Peng and Y. D. Li, *Angew. Chem. Int. Ed.*, 2005, **44**, 6054-6057.

48 Y. Lu, Y. Liu, S. Zhang, S. Wang, S. Zhang and X. Zhang, *Anal. Chem.*, 2013, **85**, 6571-6574.

49 S. Rana, N. D. B. Le, R. Mout, K. Saha, G. Y. Tonga, R. E. S. Bain, O. R. Miranda, C. M. Rotello and V. M. Rotello, *Nat. Nanotechnol.*, 2015, **10**, 65-69.